SCIENTIFIC REPORTS

OPEN

Modulated switching current density and spin-orbit torques in MnGa/Ta films with inserting ferromagnetic layers

Received: 17 June 2016
Accepted: 08 November 2016
Published: 02 December 2016

Kangkang Meng[1], Jun Miao[1], Xiaoguang Xu[1], Yong Wu[1], Jiaxing Xiao[2], Jianhua Zhao[2] & Yong Jiang[1]

We report modulated switching current density and spin-orbit torques (SOT) in MnGa/Ta films with inserting very thin Co_2FeAl and Co layers. Ferromagnetic coupling has been found in MnGa/Co_2FeAl/Ta, resulting in a decreased effective anisotropy field. On the contrary, in MnGa/Co/Ta, antiferromagnetic coupling plays a dominant role. The switching current density J_c in MnGa/Ta is 8.5×10^7 A/cm^2. After inserting 0.8-nm-thick Co_2FeAl and Co, the J_c becomes 5×10^7 A/cm^2 and 9×10^7 A/cm^2, respectively. By performing adiabatic harmonic Hall voltage measurements, it is demonstrated that the inserted Co_2FeAl layer has mainly enhanced the field-like torques, while in MnGa/Co/Ta the damping-like torques have been enhanced. Finally, the enhanced spin Hall effect (SHE) has also been studied using the spin Hall magnetoresistance measurement. The modulated J_c and SOT are ascribed to the combination of magnetic coupling, Rashba effect and SHE at the interfaces.

Spin-orbit torques (SOT) effect has been demonstrated as a promising technique to control the magnetization in heavy metal (HM)/ferromagnetic metal (FM) heterostructures[1–8]. An in-plane electric current applied to the heterostructures with large spin–orbit coupling (SOC) and structural inversion asymmetry gives rise to the torques, which induces magnetization switching under an external magnetic field collinear with the current. The torques acting on the magnetization can be represented by so-called effective magnetic fields generated by the spin Hall effect (SHE) and the Rashba effect[9–20]. When a FM contacts with a HM with strong SOC such as Ta or Pt, the charge current in the HM will be converted into pure spin current due to SHE, such spin current can diffuse into the FM layer and exert torques on its magnetization, which is similar to spin transfer torque. On the other hand, spin accumulation can also take place at the FM/HM interface via the Rashba effect, which has also generated a significant effective field that causes current-induced domain nucleation and fast domain wall (DW) motion. To evaluate the size and direction of such torques or effective fields, a number of methods have been employed. Recently, Kim *et al.* have examined the measurement of adiabatic (low-frequency) harmonic Hall voltage to study the effective fields[5]. They derived an analytical formula for the harmonic Hall voltages and found that the effective fields strongly depend on the thicknesses of Ta and CoFeB layers in Ta/CoFeB/MgO heterostructures.

For practical use of the SOT in spintronics devices, it is of great importance to elucidate the factors determining the threshold switching current density J_c. The critical current density originates from the SHE is given by $J_C = \frac{2e}{\hbar}\frac{M_S t_F}{\theta_{SH}^{eff}}\left(\frac{H_K^{eff}}{2} - \frac{H_X}{\sqrt{2}}\right)$, where H_X is an external field collinear with the current, e the elementary charge, $\hbar$ the Dirac constant, and θ_{SH}^{eff} the effective spin Hall angle. M_S, t_F and H_K^{eff} are the saturation magnetization, thickness and effective anisotropy field of the ferromagnetic layer, respectively[21]. The critical current density for the Rashba effect is given by $J_C = \frac{\hbar e H_K^{eff} M_S}{2\alpha_R m P}$, where M_S is the saturation magnetization, α_R the Rashba constant, P the electron spin polarization, and m the electron mass[22]. In a word, the switching current density is essentially determined by the characteristics of the HM and FM in the heterostructures. New paradigms for decreasing the switching current density will be possible by engineering the magnetic properties of the FM and HM/FM interfaces. On the

[1]School of Materials Science and Engineering, University of Science and Technology Beijing, Beijing 100083, China. [2]State Key Laboratory of Superlattices and Microstructures, Institute of Semiconductors, Chinese Academy of Sciences, Beijing 100083, China. Correspondence and requests for materials should be addressed to K.M. (email: kkmeng@ustb.edu.cn) or Y.J. (email: yjiang@ustb.edu.cn)

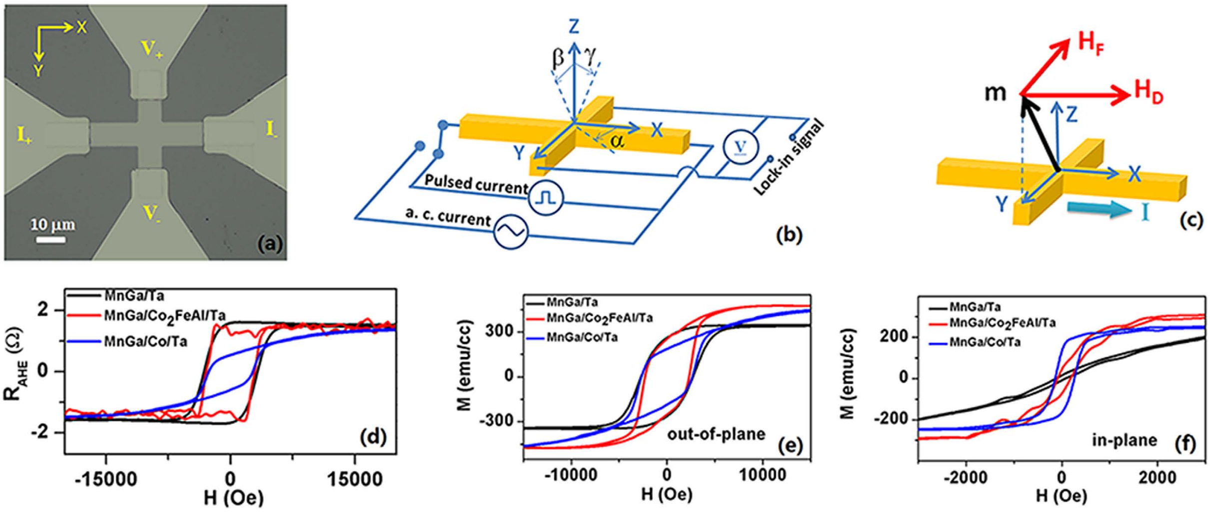

Figure 1. Device structure and magnetic properties. (**a**) SEM image of a patterned Hall bar. (**b**) Schematic measurement setup along with the definition of the coordinate system. (**c**) The corresponding field-like effective field $\mathbf{H_F}$ and damping-like effective field $\mathbf{H_D}$ when the magnetization is tilted perpendicular to the current direction. (**d**) Hysteresis loops of anomalous Hall resistance for the three samples. (**e**) Out-of-plane and (**f**) in-plane **M-H** curves of the three samples.

other hand, there are two kinds of direct exchange coupling at the interface of two FM leads: ferromagnetic and antiferromagnetic. Therefore, it provides a convenient way to modulate the magnetic properties and switching current density.

The perpendicular magnetic anisotropy (PMA) of the thin ferromagnetic films used for most of the reported SOT measurements stems from the interfacial effect[2–5]. Zhao *et al.* have also investigated the SOT induced magnetization switching in Ta/TbFeCo structures with bulk PMA[8]. Recently, we have systematically investigated the anomalous Hall effect (AHE) in $Mn_{1.5}Ga$/Ta bilayers, in which the PMA originates from bulk rather than interface, and the SOT induced magnetization switching has also been observed[23]. As an attempt to modulate the switching current density J_c and study the underlying physics, we further investigate the magnetic properties and SOT in MnGa/Ta films with inserting Co_2FeAl and Co films. Recent works have proved that the magnetic coupling in MnGa/Co_2FeAl and MnGa/Co is different, which provides a way to investigate the influence of ferromagnetic and antiferromagnetic coupling on the switching current density[24,25]. On the other hand, we select Co_2FeAl and Co as inserting layers because they have similar saturation magnetization of 1100 emu/cm^{3}and are just designed to induce different anisotropy field[26,27]. Ferromagnetic coupling has been found in MnGa/Co_2FeAl/Ta, resulting in a decreased effective anisotropy field. On the contrary, in MnGa/Co/Ta, antiferromagnetic coupling plays a dominant role. It is found that the J_c in MnGa/Ta is about 8.5×10^7 A/cm^2. After inserting a 0.8-nm-thick Co_2FeAl, J_c decreases to 5×10^7 A/cm^2. However in MnGa/Co/Ta the value is increased and even larger than that in MnGa/Ta. By performing adiabatic harmonic Hall voltage measurements, we show that the inserted Co_2FeAl layer has enhanced the effective fields, especially the field-like effective field, while the Co layer has mainly enhanced the damping-like field. The larger J_c in MnGa/Co/Ta is ascribed to its larger anisotropy field. Furthermore, the modulated SHE has also been studied using the spin Hall magnetoresistance (SMR) measurements.

Results

Device structure and current distributions. The as-prepared samples are denoted as MnGa/Ta, MnGa/Co_2FeAl/Ta, MnGa/Co/Ta and MnGa/Co/Al respectively and the Mn/Ga atomic ratio is 1[28]. A scanning electron microscope (SEM) image of a patterned Hall bar is shown in Fig. 1a. The size of all the Hall bars is 10 μm × 80 μm. The two electrodes for current injection are labelled $\mathbf{I_+}$ and $\mathbf{I_-}$. The other two electrodes for the Hall voltage measurements are labelled $\mathbf{V_+}$ and $\mathbf{V_-}$. To evaluate the perpendicular component of the magnetization and the planar Hall effect (PHE). the Hall resistance $\mathbf{R_H}$ is measured with applying a direct current (DC) of 1 mA, corresponding to a current density of around $\mathbf{j} = 1 \times 10^6$ A/cm^2. Figure 1b shows the schematic of the measurement setup along with the definition of the coordinate system used in this study. We measure the SOT induced magnetization switching by applying a pulsed current with the width 50 μs, and the resistance is measured after a 16 μs delay under an external magnetic field $\mathbf{H_X}$ along either positive or negative **X** directions. We apply a sinusoidal alternating current (AC) with the amplitude of 2.1 mA and the frequency of 158.89 Hz to exert periodic SOT on the magnetization, and the first V_ω and the second $V_{2\omega}$ harmonic anomalous Hall voltages are measured as functions of magnetic field **H** at the same time using two lock-in amplifier systems. Figure 1c shows the corresponding field-like effective field $\mathbf{H_F}$ and damping-like field $\mathbf{H_D}$ when the magnetization is tilted perpendicular to the current direction.

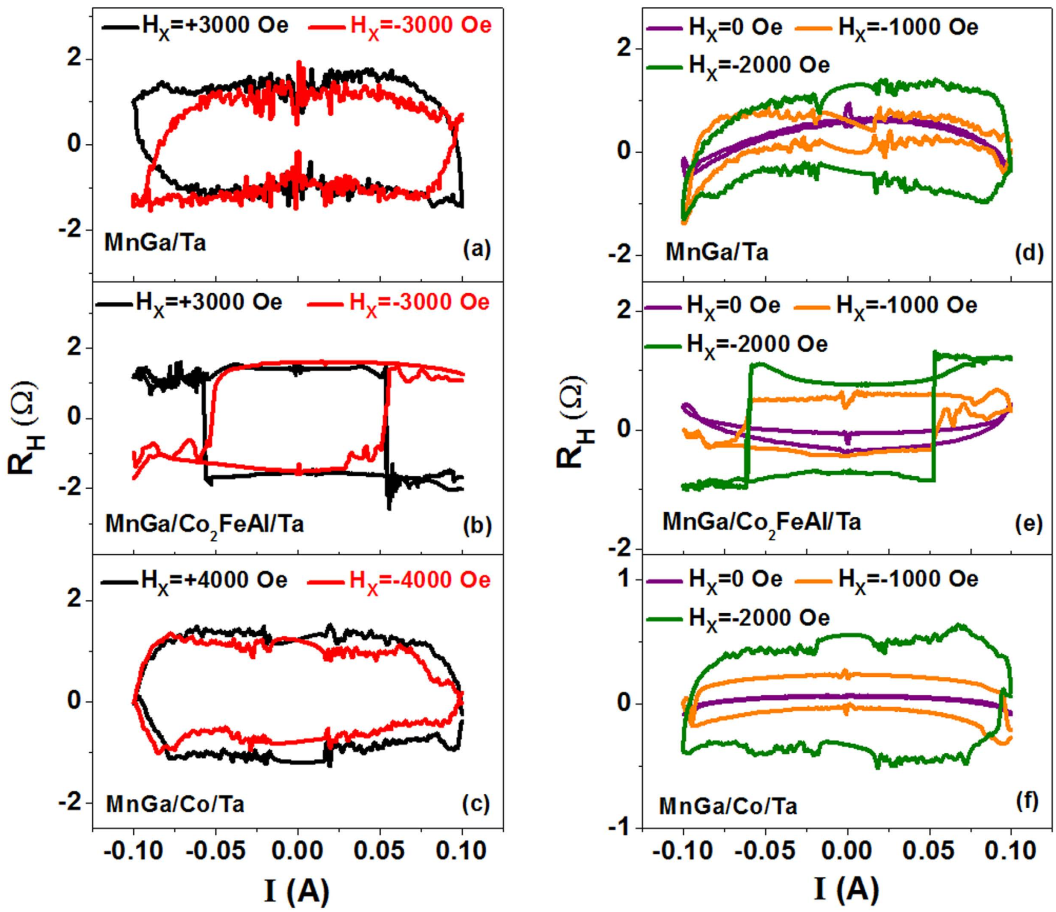

Figure 2. Current switching under in-plane magnetic field. $\mathbf{R_H}$-**I** curves of (**a**) MnGa/Ta and (**b**) MnGa/Co_2FeAl/Ta with $\mathbf{H_X} = \pm 3000$ Oe. (**c**) $\mathbf{R_H}$-**I** curves of MnGa/Co_2FeAl/Ta with $\mathbf{H_X} = \pm 4000$ Oe. (**d**–**f**) $\mathbf{R_H}$-**I** curves of the three samples with different negative $\mathbf{H_X}$.

Magnetic properties. The hysteresis loops of the AHE for MnGa/Ta, MnGa/Co_2FeAl/Ta, MnGa/Co/Ta are presented in Fig. 1d, and the anomalous Hall resistance $\mathbf{R_{AHE}}$ in all the samples are obtained by subtracting the ordinary Hall component determined from a linear fit to the high-field region up to ±6 T. We find that MnGa/Ta and MnGa/Co_2FeAl/Ta have similar PMA properties, which has also been investigated using **M-H** measurement. Figure 1e and f show the out-of-plane and in-plane **M-H** curves of the three samples, respectively. It can be found that the saturation magnetizations of both MnGa/Co/Ta and MnGa/Co_2FeAl/Ta are similar with each other but larger than that of MnGa/Ta. On the other hand, the out-of-plane **M-H** curve of MnGa/Ta in Fig. 1e is broad and not rectangle, indicating an in-plane component of magnetization at zero-field but the value is very small as shown in Fig. 1f. MnGa/Co_2FeAl/Ta shows a large saturation magnetization at high out-of-plane field, but its remnant magnetization is almost the same as that of MnGa/Ta, which could be ascribed to the ferromagnetic coupling between MnGa and Co_2FeAl[24]. On the contrary, MnGa/Co/Ta shows a small remnant magnetization and the large linear-increase of magnetization with increasing field, which indicates the antiferromagnetic coupling at the interface[25]. Both MnGa/Co_2FeAl/Ta and MnGa/Co/Ta have non-negligible in-plane components of magnetization as shown in Fig. 1f. The effective anisotropy fields of MnGa/Ta, MnGa/Co_2FeAl/Ta and MnGa/Co/Ta are calculated to be 1.5 T, 1.2 T and 1.7 T respectively using the reported method[12].

Current induced switching under H_X fields. The current-induced switching in MnGa/Ta and MnGa/Co_2FeAl/Ta with an in-plane field of $\mathbf{H_X} = \pm 3000$ Oe are shown in Fig. 2a and b, respectively. It is found that the maximum Hall resistances of the two samples are all detected at the field. The magnetization is switched from **+Z** to **−Z** with $\mathbf{H_X} = +3000$ Oe when sweeping the current from negative to positive, and switched back from **−Z** to **+Z** when sweeping the current reversely. With $\mathbf{H_X} = -3000$ Oe, the opposite switching behavior is observed. The switching current density J_c in MnGa/Ta is 8.5×10^7 A/cm^2. After inserting a 0.8-nm-thick Co_2FeAl, it decreases to 5×10^7 A/cm^2. Similar measurements are performed in MnGa/Co/Ta with the in-plane field of $\mathbf{H_X} = \pm 4000$ Oe, since the maximum Hall resistance is detected at this field. The J_c in MnGa/Co/Ta is increased to be about 9×10^7 A/cm^2. The current switching measurements are also performed over a range of in-plane external fields as shown in Fig. 2d,e. It is found that the magnetizations of the three samples are not fully switched and the anomalous Hall resistance $\mathbf{R_H}$ becomes smaller as decreasing the field, indicating that the deterministic switching gradually vanishes, which was also observed in Pt/CoNiCo/Pt symmetric devices[29]. On the other hand, the switching

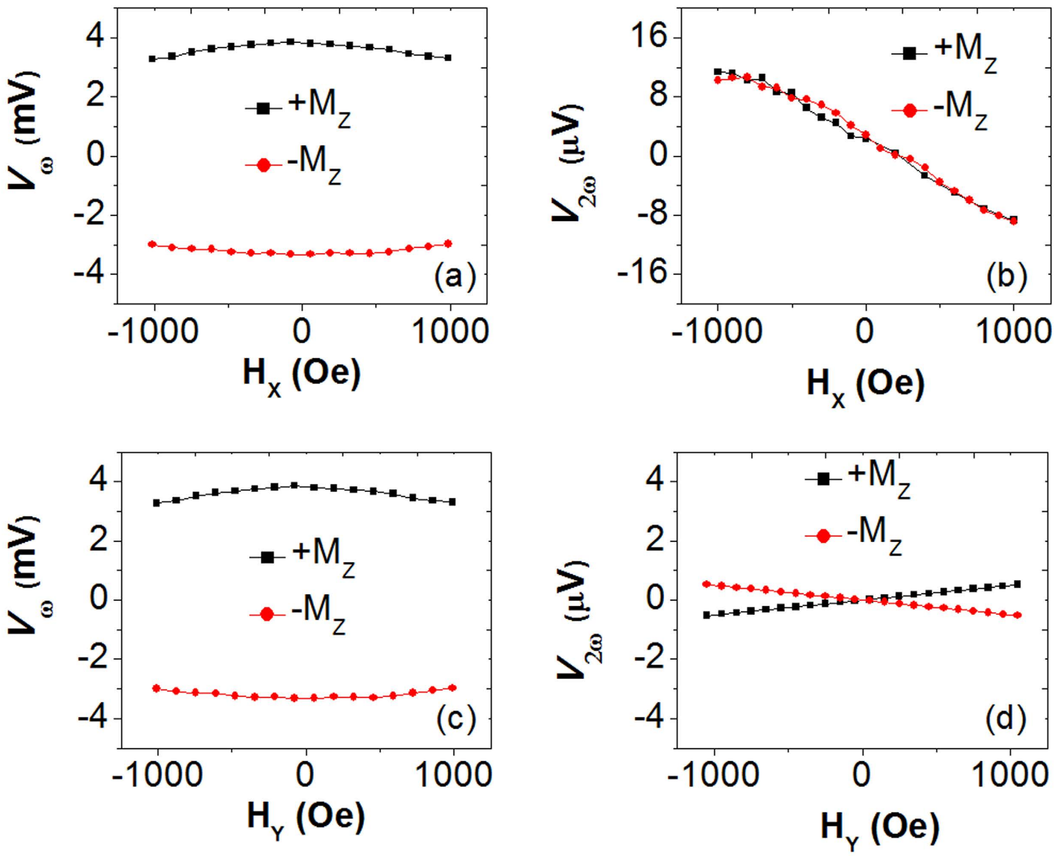

Figure 3. The harmonic results of the MnGa/Ta bilayers. (**a**) and (**b**) The first harmonic Hall voltages V_ω and the second harmonic Hall voltages $V_{2\omega}$ plotted against the in-plane external field $\mathbf{H_X}$. (**c**) and (**d**) The first harmonic Hall voltages V_ω and the second harmonic Hall voltages $V_{2\omega}$ plotted against the in-plane external field $\mathbf{H_Y}$.

behaviors of MnGa/Co/Ta with $+\mathbf{H_X}$ and $-\mathbf{H_X}$ seem to be similar. It indicates that different switching schemes happen in the sample and make the interpretation difficult, because there is evident in-plane magnetization in MnGa/Co/Ta as shown in Fig. 1f and the SOT direction may also depend on the direction of magnetization[30]. In general, the results suggest that it is easier to switch the magnetization of MnGa/Co_2FeAl/Ta as compared with MnGa/Ta but becomes hard for MnGa/Co/Ta.

Effective fields generated by the current. To determine the strength of the spin-orbit effective fields with inserting Co_2FeAl and Co layers, we have performed non-resonant magnetization-tilting measurements by applying a small amplitude low frequency alternating current through the device and simultaneously sweeping a static in-plane magnetic field parallel or perpendicular to the current direction ($\mathbf{H_X}$ and $\mathbf{H_Y}$)[4,5]. The damping-like $\mathbf{H_D}$ and field-like effective fields $\mathbf{H_F}$ can be calculated by

$$H_{D(F)} = -2\frac{\partial V_{2\omega}/\partial H_{X(Y)}}{\partial^2 V_\omega/\partial H^2_{X(Y)}}, \tag{1}$$

A diagram of the measurement is shown in Fig. 1b, where the AC current with the amplitude of 2 mA was applied along the **X** axis with the external field along **X** ($\mathbf{H_X}$, $\alpha = 0°$) and **Y** ($\mathbf{H_Y}$, $\alpha = 90°$) axis. Figure 3 shows the harmonic results of MnGa/Ta as an example. Figure 3a and b show the first harmonic Hall voltages V_ω and second harmonic Hall voltages $V_{2\omega}$ plotted against the in-plane external field $\mathbf{H_X}$, measured with the out-of-plane magnetization component $\mathbf{M_Z} > 0$ and with $\mathbf{M_Z} < 0$. Figure 3c and d show the corresponding results for $\mathbf{H_Y}$. Then, the damping-like effective field $\mathbf{H_D}$ and field-like effective field $\mathbf{H_F}$ as functions of applied current density **j** are shown in Fig. 4. The effective fields vary linearly with **j**, indicating that the effects of Joule heating are negligible in the measured **j** range. The sign of $\mathbf{H_D}$ depends on the direction of $\mathbf{M_Z}$, while that of $\mathbf{H_F}$ is independent of $\mathbf{M_Z}$, which is consistent with previous reports using the same method[4,5]. It is indicated that the inserting the Co layer has mainly enhanced the dampling-like torques while the Co_2FeAl layer has mainly enhanced the field-like torques.

Spin Hall magnetoresistance. To further investigate the modulated SHE in these samples, we have carried out the SMR measurements[31,32]. The multilayer of MnGa/Co/Al with weak SOC was fabricated as a comparison. The SMR longitudinal resistivity change can be formulated as $\rho_{xx} \approx \rho - \Delta\rho m_y^2$, where ρ is a constant resistivity

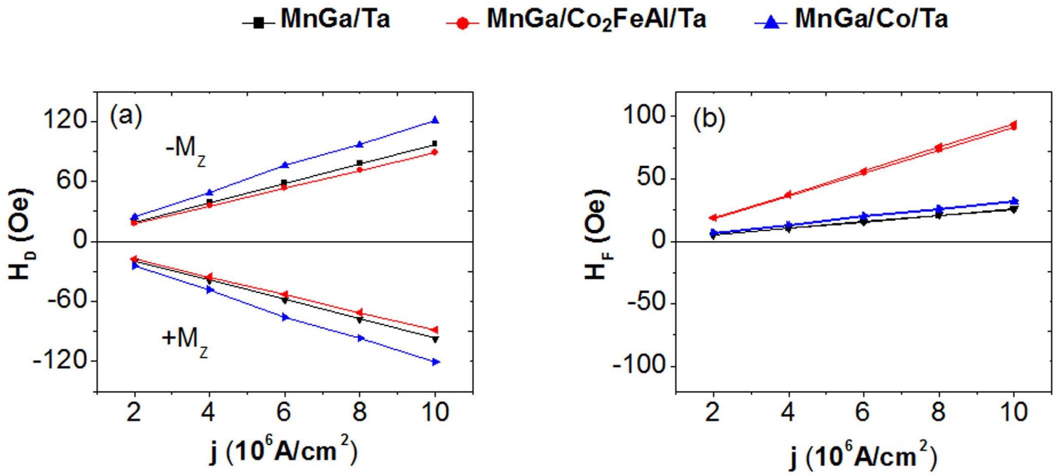

Figure 4. The effective fields deduced from harmonic results for the three samples.

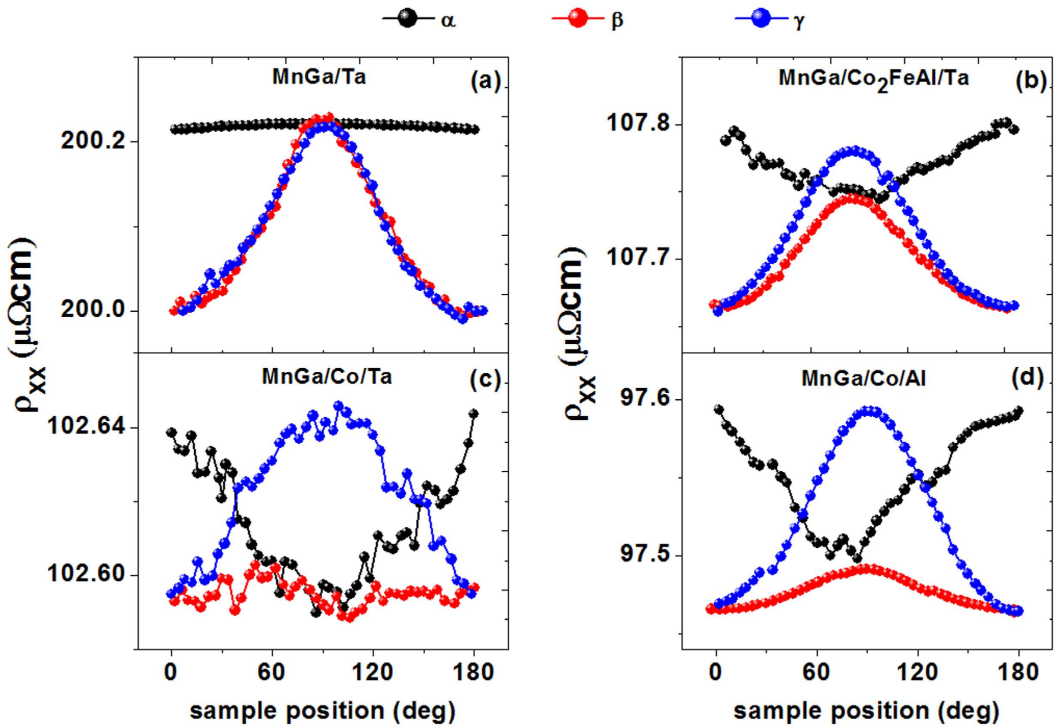

Figure 5. Angle-dependent longitudinal resistivity ρ_{XX} in three geometries for the four samples.

offset, $\Delta\rho$ the magnitude of the resistivity changes as a function of the magnetization orientation, and $\mathbf{m}_y$ the component of the magnetization in the **Y** direction that is perpendicular to the current direction in the film plane. Therefore, the SMR effect is only related to $\mathbf{m}_y$, distinct from the ordinary anisotropic magnetoresistance (AMR) effect in magnetic layers, which depends on the $\mathbf{m}_x$ component parallel to the current direction[31–33]. Figure 5 shows the angle-dependent longitudinal resistivity ρ_{XX} in three geometries for the four samples, and the applied field is 9 T. It is found that the ρ_{XX} (β) and ρ_{XX} (γ) of MnGa/Ta adapt $\sin^4$ dependence on the angles as shown in Fig. 5a, which is caused by the AMR of MnGa as investigated in our previous work[23]. After inserting Co_2FeAl layer, the ρ_{XX} (γ) also adapts $\sin^4$ dependence on the angles but the variation becomes smaller, while the ρ_{XX} (α) adapts $\sin^2$ dependence on the angles with a larger variation. For MnGa/Co/Ta, there is no obvious change on the ρ_{XX} (β) as compared with that in MnGa/Co/Al, where the SOC is weak. Here we will focus on the changes happened in ρ_{XX} (β), which indicate a different dependence on $\mathbf{m}_y$ and reveal the existence of SMR. We define the MR ratio as (ρ_{XX} ($\beta = 90°$)-ρ_{XX} ($\beta = 0°$))/ρ_{XX} ($\beta = 0°$). The MR of MnGa/Co/Ta is simply considered as the superposition of AMR and SMR, and the value is almost zero. The MR of MnGa/Co/Al is 0.026%, thus the SMR of MnGa/Co/Ta is about −0.026%. Recently, Kim *et al.* have studied the SMR in metallic HM/FM bilayers[34]. The SMR of a HM/FM bilayer reads

$$\frac{\Delta R}{R} \sim -\theta_{SH}^2 \frac{\lambda_N}{d} \frac{\tanh^2(d/2\lambda_N)}{1+\zeta} \times \left[\frac{g_R}{1+g_R \coth(d/\lambda_N)} - \frac{g_F}{1+g_F \coth(d/\lambda_N)}\right], \tag{2}$$

$$g_R \equiv 2\rho_N \lambda_N Re[G_{MIX}], \tag{3}$$

$$g_F \equiv \frac{(1-P^2)\rho_N \lambda_N}{\rho_F \lambda_F \coth(t_F/\lambda_F)}, \tag{4}$$

where ρ_N, λ_N, and θ_{SH} represent the resistivity, spin diffusion length, and spin Hall angle of the HM layer, respectively. G_{MIX} is the so-called spin mixing conductance. t_F, ρ_F, λ_F, and P represent the thickness, resistivity, spin diffusion length, and current spin polarization of the magnetic layer, respectively. The value of $\zeta \equiv (\rho_N t_F/\rho_F d)$ describes the current shunting effect into the magnetic layer. We have extracted the effective spin Hall angle $\theta_{SH} = -0.11$ of Ta in MnGa/Ta using the relationship $H_L = \hbar\theta_{SH}|j|/(2|e|M_S t_F)$, where $\mathbf{j}$ is charge current density, e the charge of an electron, M_S the saturation magnetization of MnGa, and t_F the thickness of MnGa[35]. In MnGa/Co/Ta, $P = 0.3$, $\rho_N = 125\,\mu\Omega cm$, $\theta_{SH} = -0.11$, $\lambda_N = 1.26\,nm$, $\rho_F = 385\,\mu\Omega cm$, and $t_F = 3.8\,nm$ are fixed, and Re $[G_{MIX}] = 10^{15}\,\Omega^{-1}cm^{-2}$ are assumed. λ_F is then calculated to be 2.71 nm. It shows that λ_F is larger than the thickness of the inserted Co layer, indicating less spin scattering at the MnGa/Co interface. For simplicity, in our work, the different parameters for MnGa/Co_2FeAl/Ta and MnGa/Co/Ta are only P, λ_F and ρ_F. Here $P = 0.5$, $\lambda_F = 0.8\,nm$ and $\rho_F = 314\,\mu\Omega cm$ are assumed, then the SMR of MnGa/Co_2FeAl/Ta is calculated to be −0.0008%, which is much smaller than its AMR and is hard to be distinguished.

Discussion

We have designed SOT devices based on MnGa/Ta films after inserting very thin Co_2FeAl and Co layers to study the modulated switching current density $\boldsymbol{J_c}$ and SOT. According to the band structures of Co and MnGa, the signs of the spin polarization in Co and MnGa are all negative, leading to the antiferromagnetic exchange coupling at the interface[25,36–41]. However, for Co_2FeAl in both the ordered $L2_1$ and the partially ordered $B2$ structures, the density of states number at Fermi surface for spin-up bands is larger than spin-down bands, and the spin polarization in Co_2FeAl is positive[40,41]. It is different from MnGa with negative spin polarization and the discontinuity of the band structure at the MnGa/Co_2FeAl interface becomes more pronounced, leading to a larger Rashba effect. It can also explain the smaller anisotropy and coercivity of MnGa/Co_2FeAl/Ta, because in this case the interfacial exchange coupling is ferromagnetic[24]. The ferromagnetic coupling in MnGa/Co_2FeAl has decreased the effective anisotropy field, which is one of the reasons for the decreased switching current density.

Meanwhile, the harmonic measurements have demonstrated that $\mathbf{H_F}$ was enhanced in MnGa/Co_2FeAl/Ta, which also contributes to the smaller $\boldsymbol{J_c}$. On the contrary, as mentioned above, the effective anisotropy field of MnGa/Co/Ta is larger, which makes it hard to switch the magnetization though there is a remarkable enhancement of $\mathbf{H_D}$. However, this analysis of the reversal of PMA layers by in-plane currents employs just a simple macrospin picture of magnetic dynamics. This macrospin description is clearly inadequate for providing accurate quantitative understanding of the reversal process. Lee *et al.* have studied the deterministic magnetic reversal of a perpendicularly magnetized Co layer in a Co/MgO/Ta nanosquare driven by SOT from an in-plane current flowing in a Pt under layer[18]. They have found that the reversal occurs through the nucleation of reversed domains much smaller than the device size, followed by a thermally assisted DW depinning process that results in the complete reversal of the entire Co by the DW propagation. The role of the in-plane magnetic field is to turn the in-plane orientation of the magnetic moments within the DWs to have a significant component parallel to the current flow, thereby allowing the torques from the SHE to produce a perpendicular equivalent field that can expand a reversed domain in all lateral directions. Rojas-Sánchez *et al.* have also experimentally investigated the current-induced magnetization reversal in Pt/$[Co/Ni]_3$/Al multilayers[42]. They have shown that the nucleation process occurs at the edge of the tracks carrying the charge current due to the Ørsted field. This demonstrates that the critical switching current also depends on the Ørsted field. The study of DW propagation supports the existence of a Néel DW configuration at zero field, due to the Dzyaloshinski-Moriya interaction (DMI) at the Co/Pt interface. An in-plane magnetic field is required to tune the DW center orientation along the current for efficient DW propagation. According to the magnetic properties and SMR measurements, the modulated magnetic coupling, DMI and SHE in MnGa/Co_2FeAl/Ta and MnGa/Co/Ta should also induce a variation in the domain structures and propagation, resulting in the modulated switching current density.

Furthermore, the harmonic Hall and SMR measurements have shown that the inserted Co layer has mainly enhanced the SHE, while the Co_2FeAl layer has mainly enhanced the Rashba effect. Recently, Haney *et al.* have developed semiclassical models for electron and spin transport in bilayer nanowires with a ferromagnetic layer and a nonmagnetic layer with strong SOC[43]. They have proved that the damping-like torque is typically derived from the models describing the bulk SHE and the spin transfer torque, and the field-like torque is typically derived from a Rashba model describing interfacial SOC. The SHE and Rashba interaction do not interfere with each other. That is, the interfacial spin-orbit coupling does not significantly modify the torque due to the bulk SHE. At the same time, it leads to additional torque that is closely related to those found in the two-dimensional Rashba model calculations. The inserting ultrathin Co_2FeAl or Co layers will modify both Rashba effect and SHE. It can explain the enhanced field-like torques in MnGa/Co_2FeAl/Ta mainly induced by the Rashba effect, and the enhanced damping-like torques are ascribed to the modulated SHE, which is also proved by the SMR measurement.

Lastly, as shown in Fig. 5a, the resistivity of MnGa/Ta is about 200 μΩ.cm. With measuring the resistivity of Co and Co_2FeAl layers ($\rho_{Co} = 80$ μΩcm, $\rho_{Co2FeAl} = 60$ μΩcm) directly deposited on Si/SiO_2 substrates, the current in the Ta layer is supposed to be shunted by the inserted Co or Co_2FeAl layers due to their small resistivity. The shunting effect will reduce the generated spin current in the Ta film and reduce the SHE, resulting in the increased switching current density. However, according to the harmonic Hall and SMR measurements, the SHE has been enhanced in MnGa/Co/Ta as compared with that in MnGa/Ta. Therefore, the influence of the shunting effect is smaller than that induced by the modulated SHE with varying DMI and spin mix conductance at the interface.

Although our work provides an opportunity to tune the $\boldsymbol{J}_c$ in SOT devices based on PMA MnGa, there is still much room for further theoretical and experimental works towards a better understanding of SOT and the ways to reduce the $\boldsymbol{J}_c$, which is the ultimate goal for technological applications.

Methods

In the experiment, a 3-nm-thick $L1_0$-MnGa single-crystalline film is grown on a semi-insulating GaAs (001) substrate by molecular-beam epitaxy. Then, Ta (5), Co_2FeAl (0.8)/Ta (5), Co (0.8)/Ta (5), Co (0.8)/Al (5) films (all units are in nanometers) are deposited on it by dc magnetron sputtering, respectively. On the other hand, for measuring the resistivity of Co and Co_2FeAl layers, Co_2FeAl (0.8)/Ta (5) and Co (0.8)/Ta (5) are also deposited on Si/SiO_2 substrates, respectively. Photolithography and Ar ion milling are used to pattern Hall bars and the lift-off process is used to form the contact electrodes.

References

1. Miron, I. M., Gambardella. P. *et al.* Perpendicular switching of a single ferromagnetic layer induced by in-plane current injection. *Nature*, **476,** 189–193 (2011).
2. Liu, L. Q., Pai, C.-F., Li, Y., Tseng, H. W., Ralph, D. C. & Buhrman, R. A. Spin-Torque Switching with the Giant Spin Hall Effect of Tantalum. *Science* **336,** 555 (2012).
3. Garello, K. *et al.* Symmetry and magnitude of spin-orbit torques in ferromagnetic heterostructures. *Nat. Nano*. **8,** 587–593 (2013).
4. Emori, S., Bauer, U., Ahn, S. M., Martinez, E. & Beach, G. S. D. Current-driven dynamics of chiral ferromagnetic domain walls. *Nat. Mater.* **12,** 611–616 (2013).
5. Kim, J. *et al.* Layer thickness dependence of the current-induced effective field vector in Ta/CoFeB/MgO. *Nat. Mater.* **12,** 240–245 (2013).
6. Liu, L. Q., Lee, O. J., Gudmundsen, T. J., Ralph, D. C. & Buhrman. R. A. Current-induced switching of perpendicularly magnetized magnetic layers using spin torque from the spin Hall effect. *Phys. Rev. Lett.* **109,** 096602 (2012).
7. Bhowmik, D. *et al.* Deterministic domain wall motion orthogonal to current flow due to spin orbit torque. *Sci. Rep*. **5,** 11823 (2015).
8. Zhao, Z., Jamali, M., Smith, A. K. & Wang, J.-P. Spin Hall switching of the magnetization in Ta/TbFeCo structures with bulk perpendicular anisotropy. *Appl. Phys. Lett.* **106,** 132404 (2015).
9. Avci, C. O. *et al.* Fieldlike and antidaming spin-orbit torques in as-grown and annealed Ta/CoFeB/MgO layers. *Phys. Rev. B* **89,** 214419 (2014).
10. Yu, G. *et al.* Switching of perpendicular magnetization by spin-orbit torques in the absence of external magnetic field. *Nat. Nano*. **9,** 548–554 (2014).
11. Zhang, C., Fukami, S., Sato, H., Matsukura, F. & Ohno, H. Spin-orbit torque induced magnetization switching in nano-scale Ta/CoFeB/MgO. *Appl. Phys. Lett.* **107,** 012401 (2015).
12. Fukami, S., Zhang, C. L., DuttaGupta, S., Kurenkov, A. & Ohno, H. Magnetization switching by spin-orbit torque in an antiferromagnet-ferromagnet bilayer system. *Nat. Mater.* **15,** 535–541 (2016).
13. Suzuki, T. *et al.* Current-induced effective field in perpendicularly magnetized Ta/CoFeB/MgO wire. *Appl. Phys. Lett.* **98,** 142505 (2011).
14. Qiu, X. *et al.* Spin-orbit-torque engineering via oxygen manipulation. *Nat. Nano*. **10,** 333 (2015).
15. Qiu, X. *et al.* Angular and temperature dependence of current induced spin-orbit effective fields in Ta/CoFeB/MgO nanowires. *Sci. Rep*. **4,** 4491 (2014).
16. Torrejon, J. *et al.* Current-driven asymmetric magnetization switching in perpendicularly magnetized CoFeB/MgO heterostructures. *Phys. Rev. B* **91,** 214434 (2015).
17. Fan, Y. *et al.* Magnetization switching through giant spin–orbit torque in a magnetically doped topological insulator heterostructure. *Nat. Mater.* **13,** 699–704 (2014).
18. Lee, O. J. *et al.* Central role of domain wall depinning for perpendicular magnetization switching driven by spin torque from the spin Hall effect. *Phys. Rev. B* **89,** 024418 (2014).
19. Nguyen, M.-H., Ralph, D. C. & Buhrman, R. A. Spin Torque Study of the Spin Hall Conductivity and Spin Diffusion Length in Platinum Thin Films with Varying Resistivity. *Phys. Rev. Lett.* **116,** 126601 (2016).
20. Hayashi, M., Kim, J., Yamanouchi, M. & Ohno, H. Quantitative characterization of the spin-orbit torque using harmonic Hall voltage measurements. *Phys. Rev. B* **89,** 144425 (2014).
21. Lee, K.-S., Lee, S.-W., Min, B.-C. & Lee, K.-J. Threshold current for switching of a perpendicular magnetic layer induced by spin Hall effect. *Appl. Phys. Lett.* **102,** 112410 (2013).
22. Manchon, A. & Zhang, S. Theory of nonequilibrium intrinsic spin torque in a single nanomagnet. *Phys. Rev. B* **78,** 212405 (2008).
23. Meng, K. K., Miao, J., Xu, X. G., Xiao, J. X., Zhao, J. H. & Jiang, Y. Anomalous Hall effect in $Mn_{1.5}Ga$/Ta and $Mn_{1.5}Ga$/Pt bilayers: Modification from spin-orbit coupling of heavy metals. *Phys. Rev. B* **93,** 060406(R) (2016).
24. Ma, Q. L., Mizukami, S., Zhang, X. M. & Miyazaki, T. Tunable ferromagnetic and antiferromagnetic interfacial exchange coupling in perpendicularly magnetized $L1_0$-MnGa/Co_2FeAl Heusler bilayers. *J. Appl. Phys*. **116,** 233904 (2014).
25. Ma, Q. L., Mizukami, S., Kubota, T., Zhang, X. M., Ando, Y. & Miyazaki, T. Abrupt Transition from Ferromagnetic to Antiferromagnetic of Interfacial Exchange in Perpendicularly Magnetized $L1_0$-MnGa/FeCo Tuned by Fermi Level Position. *Phys. Rev. Lett.* **112,** 157202 (2014).
26. Karanikas, J. M., Sooryakumar, R., Prinz, G. A. & Jonker, B. T. Thermal magnons in bcc cobalt-itinerancy and exchange stiffness. *J. Appl. Phys*. **69,** 6120 (1991).
27. Galanakis, I., Dederichs, P. H. & Papanikolaou, N. Slater-Pauling behavior and origin of the half-metallicity of the full-Heusler alloys. *Phys. Rev. B* **66,** 174429 (2002).
28. Zhu, L. J., Pan, D., Nie, S. H., Lu, J. & Zhao, J. H. Tailoring magnetism of multifunctional Mn_xGa films with giant perpendicular anisotropy. *Appl. Phys. Lett.* **102,** 132403 (2013).
29. Yang, M. Y. *et al.* Spin-orbit torque in Pt/CoNiCo/Pt symmetric devices. *Sci. Rep*. **6,** 20778 (2016).
30. Fukami, S., Anekawa, T., Zhang, C. & Ohno, H. A spin–orbit torque switching scheme with collinear magnetic easy axis and current configuration. *Nat. Nano.* **10,** 1038 (2016).
31. Nakayama, H. *et al.* Spin Hall Magnetoresistance Induced by a Nonequilibrium Proximity Effect. *Phys. Rev. Lett.* **110,** 206601 (2013).
32. Chen, Y.-T. *et al.* Theory of spin Hall magnetoresistance. *Phys. Rev. B* **87,** 144411 (2013).

33. Zhou, X. *et al.* Magnetotransport in metal/insulating-ferromagnet heterostructures: Spin Hall magnetoresistance or magnetic proximity effect. *Phys. Rev. B* **92,** 060402(R) (2015).
34. Kim, J., Sheng, P., Takahashi, S., Mitani, S. & Hayashi, M. Spin Hall Magnetoresistance in Metallic Bilayers. *Phys. Rev. Lett.* **116,** 097201 (2016).
35. Ramaswamy, R., Qiu, X. P., Dutta, T., Pollard, S. D. & Yang, H. Hf thickness dependence of spin-orbit torques in Hf/CoFeB/MgO heterostructures. *Appl. Phys. Lett.* **108,** 202406 (2016).
36. Winterlik, J. *et al.* Structural, electronic, and magnetic properties of tetragonal $Mn_{3-x}Ga$: Experiments and first-principles calculations. *Phys. Rev. B* **77,** 054406 (R) (2008).
37. Mizukami, S. *et al.* Long-Lived Ultrafast Spin Precession in Manganese Alloys Films with a Large Perpendicular Magnetic Anisotropy. *Phys. Rev. Lett*. **106,** 117201 (2011).
38. Schwarzt, K., Mohnt, P., Blahat, P. & Kubler, J. Electronic and magnetic structure of BCC Fe-Co alloys from band theory. *J. Phys. F* **14,** 2659 (1984).
39. Coey, J. M. D. *Magnetism and Magnetic Materials* (Cambridge University Press, Cambridge, England, 2010), Chap. 5.
40. Miura, Y., Nagao, K. & Shirai, M. Atomic disorder effects on half-metallicity of the full-Heusler alloys $Co_2(Cr_{1-x}Fe_x)$ Al: A first-principles study. *Phys. Rev. B* **69,** 144413 (2004).
41. Fecher, G. H. & Felser, C. Substituting the main group element in cobalt–iron based Heusler alloys: $Co_2FeAl_{1-x}Si_x$. *J. Phys. D: Appl. Phys*. **40,** 1582–1586 (2007).
42. Rojas-Sánchez *et al.* Perpendicular magnetization reversal in Pt/$[Co/Ni]_3$/Al multilayers *via* the spin Hall effect of Pt. *Appl. Phys. Lett.* **108,** 082406 (2016).
43. Haney, P. M., Lee, H.-W., Lee, K.-J., Manchon, A. & Stiles, M. D. Current induced torques and interfacial spin-orbit coupling: Semiclassical modeling. *Phys. Rev. B* **87,** 174411 (2013).

Acknowledgements
This work was partially supported by the National Basic Research Program of China (2015CB921502), the National Science Foundation of China (Grant Nos 61404125, 51371024, 51325101, 51271020).

Author Contributions
K.K.M. and Y.J. conceived and designed the study. K.K.M. and J.X.X. carried out the sample preparation and testing. Y.W., X.G.X. and J.M. gave out the amendments for manuscript. J.H.Z. contributed to the scientific discussions. All authors reviewed the manuscript.

Additional Information
Competing financial interests: The authors declare no competing financial interests.

How to cite this article: Meng, K. *et al.* Modulated switching current density and spin-orbit torques in MnGa/Ta films with inserting ferromagnetic layers. *Sci. Rep.* **6**, 38375; doi: 10.1038/srep38375 (2016).